

# SOME OBSERVATIONS OF THE BEHAVIOR OF SPHERICAL HARMONIC WAVES\*

RAYMOND J. DELAND

New York University, New York, N.Y.

## ABSTRACT

One month of daily spherical harmonic expansions of 500-mb. height in the Northern Hemisphere were studied. The movements of the waves are compared with the Rossby-Haurwitz wave speeds computed from the zonal geostrophic wind profile. Systematic differences between the observed and theoretical wave speeds are found.

## 1. INTRODUCTION

The description of the isobaric and stream-function fields in terms of surface-spherical harmonics is of special interest because the latter are characteristic functions of the nonlinear vorticity equation. The speed of movement of these spherical-harmonic waves can therefore be theoretically calculated (assuming nondivergence) without the assumption of small amplitude that underlies the familiar Rossby wave speed. There have been many theoretical studies of the behavior of the spherical-harmonic waves (Neamtan [12], Haurwitz and Craig [7], Silberman [15], Platzman [13], [14], Kubota [9]) and some papers on numerical prediction using spherical-harmonic expansions (Baer and Platzman [2] and Baer [1]), but so far very little evidence on the behavior of spherical-harmonic expansions of real fields has appeared in the literature.

Dr. H. W. Ellsaesser of the Lawrence Radiation Laboratory, Livermore, has kindly provided me with daily computations, for April 1960, of spherical-harmonic expansions of the 500-mb. height over the Northern Hemisphere, and some aspects of the behavior of these are presented in this paper. A month is a relatively small sample, so that there is considerable statistical uncertainty in the results, but it appears to be sufficient for some conclusions to be drawn from it. The results are relevant to the experiments with numerical prediction using spherical harmonics, in fact they present some interesting contrasts with the results of Baer's [1] computations.

## 2. BASIC FORMULAS

The height of the isobaric surface, as a function of latitude, longitude, and time, is expressed as

$$\Psi(\lambda, \mu, t) = \sum_{m,n} \Psi_n^m(t) P_n^m(\mu) e^{im\lambda} \quad (1)$$

where  $\lambda$  is longitude;  $\mu = \sin \varphi$ , where  $\varphi$  is latitude;  $m$  is longitudinal wave number (also called the "rank");  $n$  is the degree of the harmonic ( $n-m$  is similar to a wave number of latitudinal variation);  $P_n^m$  is the normalized associated Legendre polynomial of rank  $m$  and degree  $n$ , and  $\Psi_n^m(t)$  is the (complex) amplitude of the particular harmonic.

The reader is referred to the papers of Haurwitz and Craig [7] and Silberman [15] for detailed discussions of the spherical-harmonic representation of geophysical fields.

When working with only one hemisphere of data only half the full number of harmonics is necessary. For those considered here ( $n-m$ ) takes odd values only. These "odd harmonics" are realistic in that they all have zero amplitude at the equator, while the implied anti-symmetric Southern Hemisphere may be ignored as a mathematically necessary but physically inconsequential addition to Northern Hemisphere fields.

Platzman [14] has shown that the nondivergent vorticity equation leads to the following expression for the phase speed; i.e., the change of phase with time, which is equivalent to the speed of movement of the wave:

$$\omega_\lambda = \frac{1}{2} \int_{-1}^1 (P_\lambda)^2 \left( \hat{\Omega}(\mu) - \frac{1}{n_\lambda(n_\lambda+1)} \frac{d\hat{\zeta}}{d\mu} \right) d\mu - \frac{1}{m_\lambda} \sum_{\beta, \alpha} I_{\lambda, \beta, \alpha} \operatorname{Re} (\bar{\zeta}_\lambda \zeta_\beta \zeta_\alpha) |\zeta_\lambda|^{-2} \quad (2)$$

where  $\lambda$ ,  $\beta$ , and  $\alpha$  represent three different ( $m$ ,  $n$ ) pairs,  $m_\lambda$  and  $n_\lambda$  are the rank and degree of the  $\lambda$ -harmonic,  $\zeta_\lambda$  is the absolute vorticity associated with the particular harmonic  $\lambda$ ,  $\hat{\zeta}$  is the zonally averaged absolute vorticity,  $\hat{\Omega}(\mu)$  is the absolute angular velocity of the zonally averaged flow, and  $I_{\lambda, \beta, \alpha}$  represents a coefficient of interaction. The earth's radius and the reciprocal of the angular velocity of the earth are the units of length and time respectively.

In equation (2), the integral is the contribution of the zonal wind speed and the earth's rotation to the total wave speed, and might reasonably be called the Rossby-

\*Contribution No. 29, Geophysical Sciences Laboratory of the Department of Meteorology and Oceanography, New York University.

Haurwitz wave speed. It is called the "convective wave speed" by Platzman [14]. The second term is the sum of the effects of all the interactions with other waves, and is called the "eddy phase speed" by Platzman.

### 3. ANALYSIS OF THE DATA

When the lower harmonics are plotted on a polar diagram as in figure 1, it is immediately apparent that the wave vector does not describe a circle around the pole as it would in the case of a single moving wave, but instead follows an eccentric circular path as if it represented the sum of a more or less fixed wave and a traveling wave. This two-component model of the lowest harmonics has been discussed by Deland [4] when analyzing zonal Fourier harmonics. Figure 1 is a better illustration of this behavior than was obtained from the Fourier zonal harmonics, for reasons that will be apparent later.

Because of the eccentric circular motion of the lower harmonics, the wave speeds were determined from the analysis of the angle  $\Delta\alpha$  (see fig. 1). For uniform circular motion, eccentric or not,  $\Delta\alpha$  would be constant and the speed of movement of the moving wave would be

$$\omega = \Delta\alpha \text{ radians (of phase) day}^{-1}$$

$$= \frac{\Delta\alpha}{m} \frac{360}{2\pi} \text{ deg. long. day}^{-1} \quad (3)$$

Note that since the phase changes by  $360^\circ$  while the longitudinal "position" of the wave (e.g., the longitude of a maximum) changes by  $360^\circ/m$ , the longitudinal speed is equal to (phase speed)/ $m$ . In the case of centered circular motion (traveling component only),  $\Delta\alpha = \Delta\varphi$ , where  $\varphi$  is the phase of the harmonic. For the smaller-scale waves there is negligible difference between the behavior of  $\Delta\alpha$  and  $\Delta\varphi$ .

Large and erratic values of  $\Delta\alpha$  occur especially often when the actual change in the wave is small. These seem to be for the most part unrepresentative. Accordingly, the representative wave speed was estimated by weighting the speed by the magnitude of the vector change according to the formula:

$$\bar{\omega} = \frac{360}{2\pi m} \left( A_1 + 2 \sum_{i=2}^{28} A_i + A_{29} \right)^{-1} \sum_{i=2}^{29} \Delta\alpha_i (A_{i-1} + A_i) \text{ deg. long. day}^{-1} \quad (4)$$

See figure 1 for the meanings of the symbols. For a qualitative check on the reliability of this procedure, the values of  $\Delta\alpha$  were in each case classified in  $10^\circ$  classes and plotted in the form of a frequency diagram. The frequency diagrams for some of the cases considered are reproduced in figure 2, with the average wave speed indicated. The average wave speed agrees quite well with the mode of the distributions in most cases, with some exceptions that will be discussed later.

The integral in equation (2) was numerically integrated

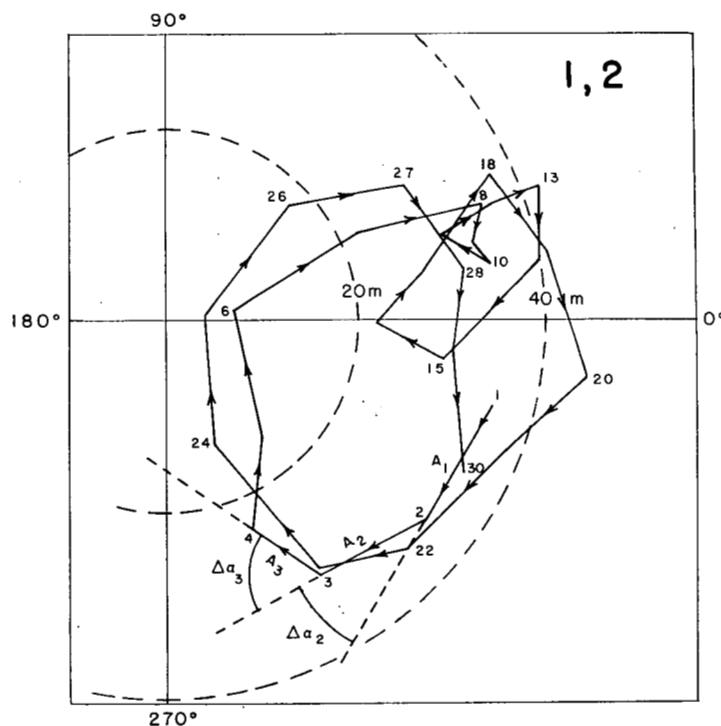


FIGURE 1.—Polar diagram for the harmonic (1,2), each point representing one day. Amplitude in meters, phase increasing anticlockwise in same sense as longitude east of Greenwich, with zero phase corresponding to a maximum at the Greenwich meridian.

using the mean (for April 1960) zonal profile of geopotential and the geostrophic assumption. The values of the weighting factor  $(P_i)^2$  were determined from the graphs, tables, and coefficients published in Jahnke and Emde [8], the Mathematical Tables Project [11], and Egersdörfer and Egersdörfer [5] respectively (in order of increasing complexity and decreasing convenience of use—one goes as far as one can with each in turn). The two parts of the integral were evaluated separately; the details are given in the Appendix.

The calculations were made for longitudinal wave numbers 1–10, for the first four values of  $n-m$ , except for  $m=1$  and 2, for which the speeds were evaluated for five degrees each. For each wave number the highest degree considered here corresponds roughly to a latitudinal half-wavelength of  $20^\circ$ – $25^\circ$  latitude. The computations were carried out up to  $m=10$  only, partly because the estimation of average speeds is increasingly uncertain as the wave number increases beyond 10 and speeds increase (see discussion of  $m=10$  later in the paper).

Average observed speeds, and theoretical speeds estimated as explained above, are shown in table 1. Average amplitudes of the observed waves are also shown in the table. It is apparent from the latter that the computations here presented were not carried out to small enough scales to include all the waves that contribute significantly to the total variation, but the important waves are included.

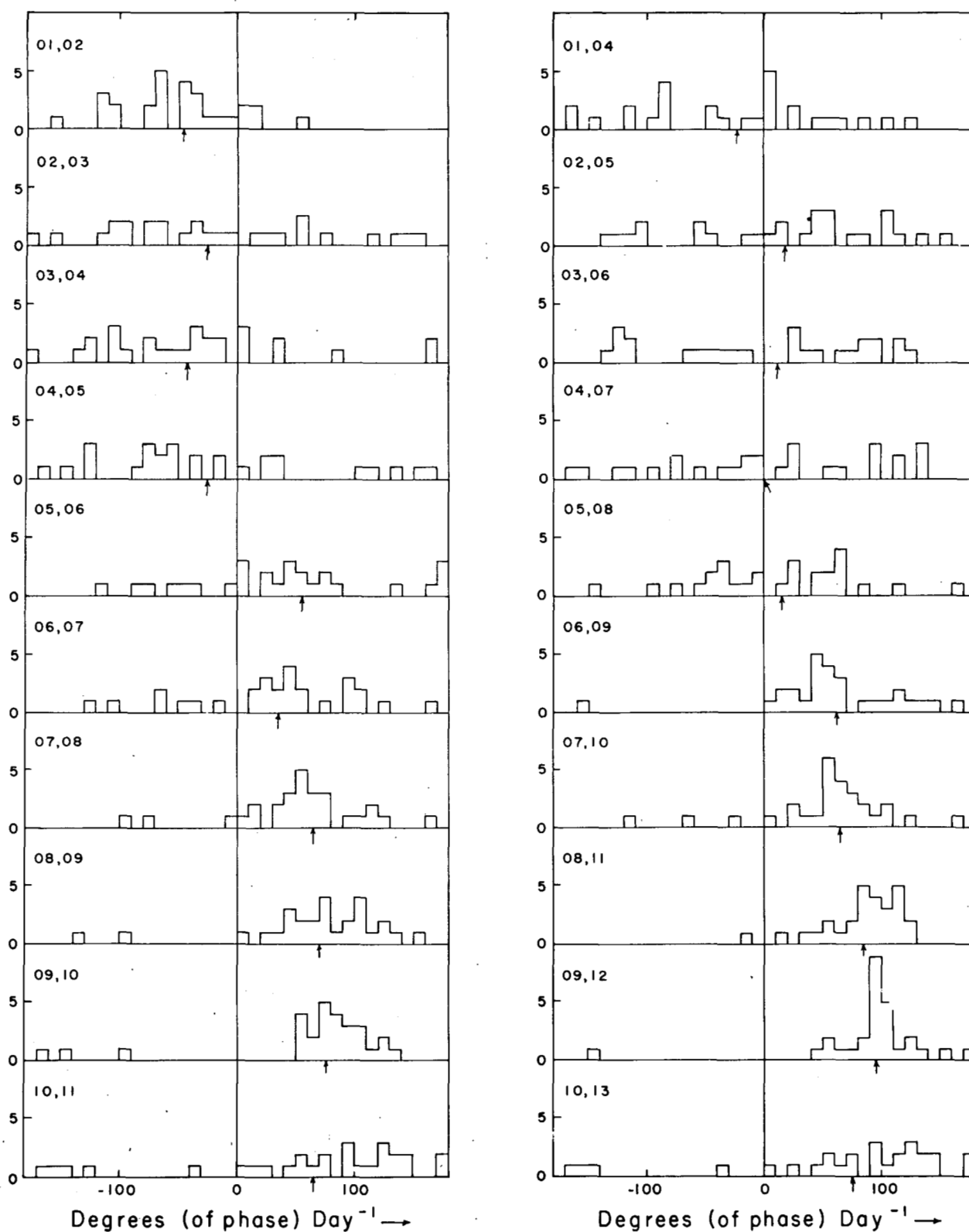


FIGURE 2.—Frequency diagrams for the angle  $\Delta\alpha$  (see fig. 1 for specification) for  $m=1-10$ ,  $n=m+1$  and  $m+3$ . Corresponding mean wave speeds are indicated by arrow.

TABLE 1.—Theoretical and observed wave speeds (in degrees of longitude per day)

|          | Longitudinal wave number |                 |                 |                |                |                |                 |                 |                 |                  |
|----------|--------------------------|-----------------|-----------------|----------------|----------------|----------------|-----------------|-----------------|-----------------|------------------|
|          | 1                        | 2               | 3               | 4              | 5              | 6              | 7               | 8               | 9               | 10               |
| Adv..... | (1, 2)<br>12.0           | (2, 3)<br>11.6  | (3, 4)<br>10.9  | (4, 5)<br>9.9  | (5, 6)<br>10.9 | (6, 7)<br>8.6  | (7, 8)<br>7.7   | (8, 9)<br>6.8   | (9, 10)<br>6.4  | (10, 11)<br>5.8  |
| R-H..... | -114.7                   | -53.4           | -28.5           | -15.5          | -7.1           | -5.5           | -2.5            | -0.9            | 0.2             | 0.7              |
| Obs..... | -47.2                    | -11.8           | -13.7           | -6.2           | 10.8           | 5.8            | 8.1             | 8.7             | 8.5             | 6.4              |
| Amp..... | 29.8                     | 15.2            | 14.1            | 14.7           | 14.5           | 10.9           | 8.8             | 6.3             | 4.2             | 3.3              |
| Adv..... | (1, 4)<br>9.2            | (2, 5)<br>8.8   | (3, 6)<br>9.3   | (4, 7)<br>9.8  | (5, 8)<br>10.5 | (6, 9)<br>11.1 | (7, 10)<br>11.4 | (8, 11)<br>11.1 | (9, 12)<br>10.5 | (10, 13)<br>10.4 |
| R-H..... | -24.8                    | -12.8           | -6.7            | -3.2           | -1             | 2.0            | 4.9             | 4.7             | 5.2             | 5.9              |
| Obs..... | -21.7                    | 8.2             | 3.6             | 1              | 3.6            | 10.5           | 9.1             | 10.7            | 10.4            | 7.4              |
| Amp..... | 39.1                     | 30.7            | 16.5            | 17.9           | 21.1           | 17.2           | 13.1            | 9.7             | 7.8             | 5.4              |
| Adv..... | (1, 6)<br>10.3           | (2, 7)<br>9.6   | (3, 8)<br>8.2   | (4, 9)<br>9.4  | (5, 10)<br>9.3 | (6, 11)<br>9.6 | (7, 12)<br>10.2 | (8, 13)<br>10.5 | (9, 14)<br>10.7 | (10, 15)<br>10.9 |
| R-H..... | -7.7                     | -3.3            | -2              | 1.8            | 3.3            | 4.3            | 5.5             | 6.3             | 7.0             | 7.6              |
| Obs..... | -14.2                    | -4              | 14.6            | 11.2           | 7.1            | 11.9           | 10.7            | 12.5            | 10.6            | 8.9              |
| Amp..... | 22.9                     | 21.7            | 19.7            | 17.2           | 12.2           | 12.6           | 10.5            | 7.8             | 7.9             | 5.5              |
| Adv..... | (1, 8)<br>10.0           | (2, 9)<br>9.2   | (3, 10)<br>10.0 | (4, 11)<br>8.5 | (5, 12)<br>8.9 | (6, 13)<br>9.6 | (7, 14)<br>9.3  | (8, 15)<br>9.8  | (9, 16)<br>10.8 | (10, 17)<br>10.8 |
| R-H..... | 3                        | 1.4             | 3.1             | 3.8            | 5.0            | 6.2            | 6.3             | 7.0             | 7.7             | 7.9              |
| Obs..... | -1.3                     | 4.3             | 10.7            | 11.1           | 14.6           | 12.4           | 12.1            | 13.3            | 10.1            | 8.8              |
| Amp..... | 25.6                     | 17.5            | 12.8            | 14.1           | 7.0            | 9.3            | 6.3             | 5.5             | 4.8             | 3.7              |
| Adv..... | (1, 10)<br>10.4          | (2, 11)<br>11.7 |                 |                |                |                |                 |                 |                 |                  |
| R-H..... | 4.7                      | 6.5             |                 |                |                |                |                 |                 |                 |                  |
| Obs..... | 24.3                     | 17.0            |                 |                |                |                |                 |                 |                 |                  |
| Amp..... | 10.3                     | 14.6            |                 |                |                |                |                 |                 |                 |                  |

Adv. = Advective part (see Appendix) of R-H speed.  
R-H = Theoretical nondivergent (Rossby-Haurwitz) speed.  
Obs. = Observed weighted average speed.  
Amp. = Average amplitude of harmonic in meters.

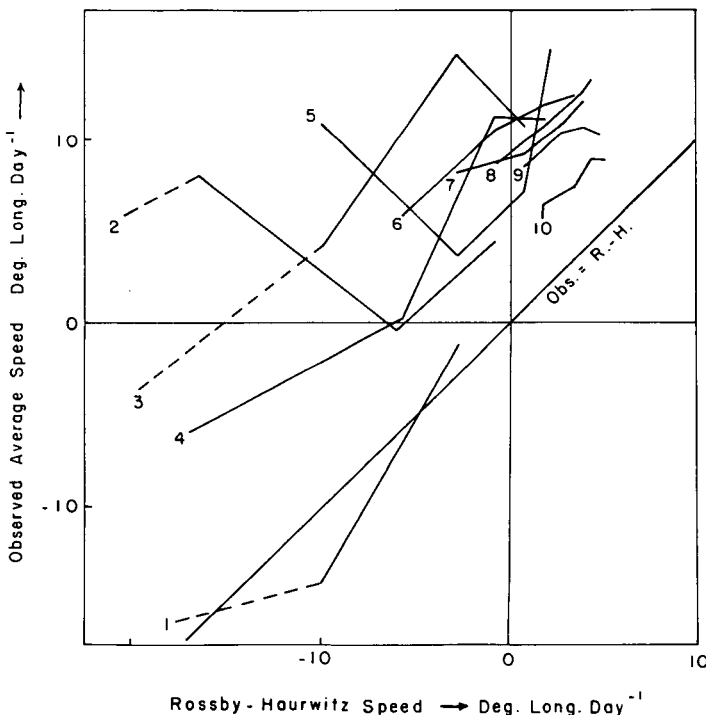


FIGURE 3.—Observed mean wave speeds plotted against Rossby-Haurwitz wave speeds. The points for each longitudinal wave number are joined by straight lines in order of increasing  $n$  (decreasing latitudinal scale) with the longitudinal wave number printed near the first point ( $m, m+1$ ). The large negative speeds for wave numbers 1, 2, and 3 are omitted.

The observed average speeds are plotted against the Rossby-Haurwitz speeds in figure 3, omitting the large negative wave speeds for  $m=1, 2$ , and 3. The corresponding average phase differences (equal to  $m$  times the average speed) are indicated on the frequency diagrams in figure 2.

#### 4. DISCUSSION

The westward movement of the waves of greatest scale, noticed by Kubota and Iida [10] and recently discussed by Deland [4], is very well shown by these data (especially for  $\Psi_2^1$ ; see fig. 1). The retrogressions of  $\Psi_2^1$  and  $\Psi_3^2$ , the lowest degrees of the two longest waves, though rapid, are not as rapid as predicted by the nondivergent vorticity equation. It is of interest that the larger westward wave speeds of the Fourier zonal harmonics found previously (Deland [4]) agree very well with the Rossby-Haurwitz wave speeds, but this may be coincidence.

All the waves show greater eastward, or less rapid westward, motion than would be predicted from the Rossby-Haurwitz wave speed. The variation with degree (i.e., with respect to latitudinal scale) for each longitudinal wave number is approximately in accordance with the nondivergent Rossby-Haurwitz wave speed. An elegant illustration of the variation of speed with latitudinal scale is the case of longitudinal wave number 3—the lowest degree moves westward while the higher degrees move eastward (see figs. 3 and 4). This is believed to be the first time the much-predicted variation

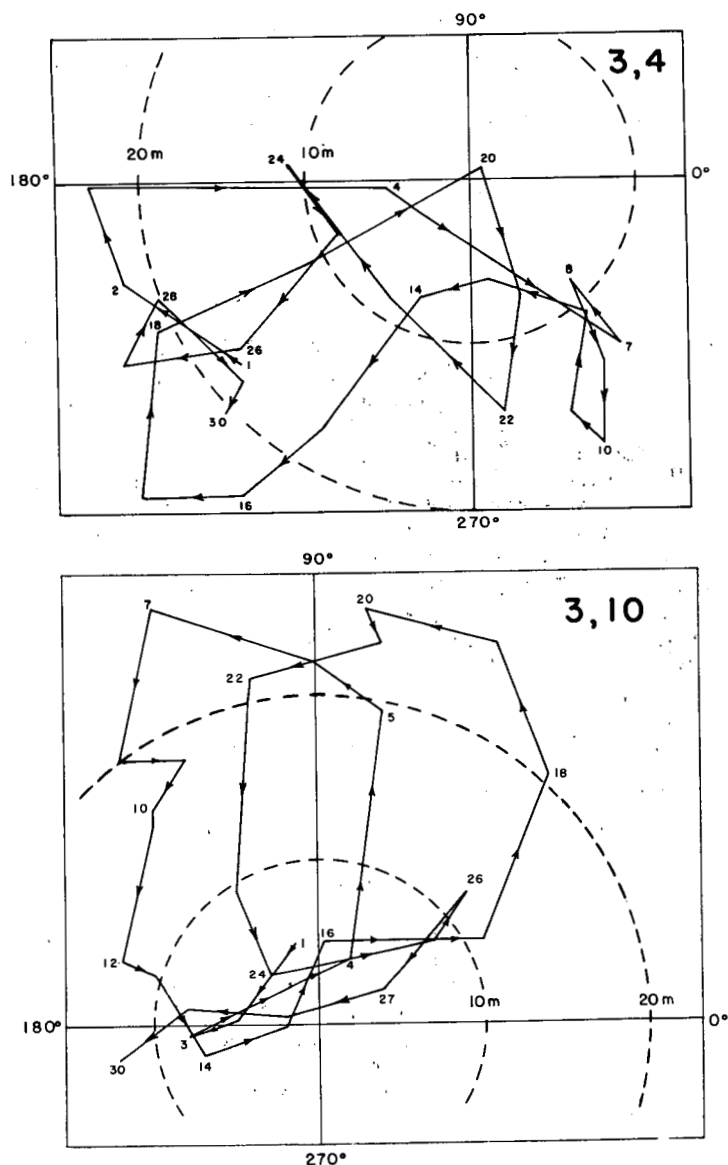


FIGURE 4.—Daily values of the harmonics (3,4) and (3,10) plotted on polar diagrams. Otherwise the same as for figure 1.

of speed with latitudinal scale has been shown to exist for actual observed waves.

For the lowest degree of each of the higher wave numbers, such as  $\Psi_{10}^9$ , the Rossby-Haurwitz wave speeds are especially small, compared to their values for other harmonics. This is apparently because the greatest weighting of the zonal wind speed in the integral in equation (2) shifts into low latitudes where the zonal wind is less, as the wave number increases. These low Rossby-Haurwitz wave speeds are particularly unrealistic compared to the observed wave motions.

In the case of wave number 10 the frequency diagrams in figure 2 show a relatively small number of occurrences of small negative values and a relatively large number of large negative values near  $-180^\circ$ . Bearing in mind

that we cannot distinguish between an angle  $\theta$  and its "negative complement" ( $\theta - 2\pi$ ), it appears that these large negative values correspond to eastward movements of more than  $180^\circ$  in phase, i.e.,  $18^\circ$  of longitude for wave number 10. The left-hand end of the frequency distribution apparently is the extension of the right-hand end. The misinterpretation of those movements in the mean wave-speed computation leads to underestimation of the wave speed. A similar observation was made by Eliassen [6] in analyzing Fourier zonal harmonics.

A noteworthy feature of the observed wave motions is their approximate agreement with the predictions of the nondivergent vorticity equation throughout the entire range of wave numbers. This is of considerable interest in relation to Burger's [3] conclusion that the vorticity equation loses its dynamic nature for planetary-scale motions. The ultra-long traveling waves apparently do not belong in the category of Burger's planetary waves, aside from being disqualified in any case for moving.

Why do the waves considered here move so fast toward the east, including the retrogressing waves of greatest scale, whose westward speed is less than expected from the nondivergent vorticity equation? There are many possible explanations, and it is certainly not necessary to assume that one explanation suffices for all scales, but it is possible that they are all carried along by the faster-moving smaller-scale waves, by means of the nonlinear interactions. One could consider the presumably random (in this respect) interactions as "turbulence" in the two-dimensional rank-and-degree domain, tending to "mix" the wave velocities to a uniform value. This hypothesis can only be tested, of course, by using more complete models such as that of Baer [1].

#### APPENDIX: COMPUTATION OF ROSSBY-HAURWITZ WAVE SPEEDS

The integral in equation (2) was split into two parts

$$A. \quad \frac{1}{2} \int_{-1}^1 (P_\lambda)^2 \hat{\Omega}(\mu) d\mu$$

$$B. \quad -\frac{1}{2} c_\lambda \int_{-1}^1 (P_\lambda)^2 \frac{d\hat{\omega}}{d\mu} d\mu, \quad c_\lambda = \frac{1}{n_\lambda(n_\lambda + 1)}$$

A. Since  $\mu \equiv \sin \varphi$ , and  $\hat{\Omega}(\mu) = \Omega + \hat{\omega}(\mu)$  where  $\Omega$  is the constant angular velocity of the earth and  $\hat{\omega}(\mu)$  is the angular velocity of the average zonal wind, the integral can be written

$$\begin{aligned} & \frac{1}{2} \int_{-\pi/2}^{\pi/2} (P_\lambda)^2 \{ \Omega + \hat{\omega}(\mu) \} \cos \varphi d\varphi \\ &= \Omega + \frac{1}{2} \int_{-\pi/2}^{\pi/2} \hat{\omega}(\mu) (P_\lambda)^2 \cos \varphi d\varphi \end{aligned}$$

since

$$\int_{-\pi/2}^{\pi/2} (P_\lambda)^2 \cos \varphi d\varphi = 2$$

(as long as we use the normalization of the harmonics given by Platzman [14]).

Subtracting  $\Omega$  we have

$$\frac{1}{2} \int_{-\pi/2}^{\pi/2} \hat{\omega}(\mu) (P_\lambda)^2 \cos \varphi d\varphi$$

as the "advective" contribution to the relative wave speed. Its value is listed separately in table 1.

The integral was numerically integrated as

$$\sum (P_\lambda)^2 \cos \varphi \hat{\omega}(\varphi) \Delta \varphi,$$

with small end corrections, with  $\Delta \varphi = 10^\circ$  for the lower-degree, smoother, harmonics and  $5^\circ$  for the higher-degree harmonics. An approximate check on the integration procedure is given by the requirement that

$$\sum_{\varphi=0}^{\pi/2} (P_\lambda)^2 \cos \varphi \Delta \varphi \approx 1, \Delta \varphi \text{ in radians.}$$

$\hat{\omega}(\mu)$  was evaluated as  $\frac{\hat{U}(\varphi)}{a \cos \varphi}$ , where  $\hat{U}(\varphi)$  is the zonal

wind speed and  $a$  is the radius of the earth.  $\hat{U}(\varphi)$  was determined by differencing over  $5^\circ$  latitude the monthly average height profile, assuming geostrophic winds. With  $\hat{U}(\varphi)$  in m. sec.<sup>-1</sup> and  $a$  in meters, the speed is expressed in radians per second and was then multiplied by  $(86,400 \times 360)/2\pi$  to bring it to degrees of longitude per day.

B. Again with the anti-symmetric assumption, the integral was expressed as

$$-\frac{1}{c_\lambda} \int_{\zeta(\text{equator})}^{\zeta(\text{pole})} (P_\lambda)^2 d\zeta$$

$\hat{\zeta} = f + \zeta_{\text{rel}}$  was evaluated at  $10^\circ$  and  $5^\circ$  latitude intervals, and the integral expressed as

$$-\frac{1}{c_\lambda} \sum_E^P (P_\lambda)^2 \Delta \hat{\zeta},$$

again with estimated end corrections, which are somewhat uncertain in this case but in no case affect the results significantly. The conversion to degrees of longitude per day is straightforward.

## ACKNOWLEDGMENTS

I would like to thank Dr. H. W. Ellsaesser for computing the spherical harmonics, and Messrs. Donald Johnson and Charles Hutchins for supplying the zonal mean heights. The study was supported in part by the U.S. Weather Bureau, Grant IWBG 10-Project 4.

## REFERENCES

1. F. Baer, "Integration with the Spectral Vorticity Equation," *Journal of the Atmospheric Sciences*, vol. 21, No. 3, May 1964, pp. 260-276.
2. F. Baer and G. W. Platzman, "A Procedure for Numerical Integration of the Spectral Vorticity Equation," *Journal of Meteorology*, vol. 18, No. 3, June 1961, pp. 393-401.
3. A. P. Burger, "Scale Consideration of Planetary Motions of the Atmosphere," *Tellus*, vol. 10, No. 2, May 1958, pp. 195-205.
4. R. J. Deland, "Traveling Planetary Waves," *Tellus*, vol. 16, No. 2, May 1964, pp. 271-273.
5. R. and L. Egersdörfer, "Formeln und Tabellen der zugeordneten Kugelfunktionen 1. Art. von  $n=1$  bis  $n=20$ . I. Teil: Formeln," *Wissenschaftliche Abhandlungen*, vol. 1, No. 6, Deutsches Reich, Reichsamt für Wetterdienst, 1936.
6. E. Eliassen, "A Study of the Long Atmospheric Waves on the Basis of Zonal Harmonic Analysis," *Tellus*, vol. 10, No. 2, May 1958, pp. 206-215.
7. B. Haurwitz and R. A. Craig, "Atmospheric Flow Patterns and Their Representation by Spherical-Surface Harmonics," *Geophysical Research Papers* No. 14, Geophysics Research Directorate, Air Force Cambridge Research Center, 1952.
8. E. Jahnke and F. Emde, *Tables of Functions*, Dover Publications, New York, 1945.
9. S. Kubota, "Surface Spherical Harmonic Representations of the System of Equations for Analysis," *Papers in Meteorology and Geophysics*, Tokyo University, vol. 10, 1960, pp. 145-166.
10. S. Kubota and S. Iida, "Statistical Characteristics of the Atmospheric Disturbances," *Papers in Meteorology and Geophysics*, Tokyo University, vol. 5, 1954, pp. 22-34.
11. Mathematical Tables Project, *Tables of Associated Legendre Functions*, Columbia University Press, New York, 1945.
12. S. M. Neamtan, "The Motion of Harmonic Waves in the Atmosphere," *Journal of Meteorology*, vol. 3, No. 2, June 1946, pp. 53-56.
13. G. W. Platzman, "The Spectral Form of the Vorticity Equation," *Journal of Meteorology*, vol. 17, No. 6, Dec. 1960, pp. 635-644.
14. G. W. Platzman, "The Analytical Dynamics of the Spectral Vorticity Equation," *Technical Report* No. 10 to National Science Foundation (Grant NSF-G2169), the University of Chicago, Department of the Geophysical Sciences, 1962.
15. I. Silberman, "Planetary Waves in the Atmosphere," *Journal of Meteorology*, vol. 11, No. 1, Feb. 1954, pp. 27-34.

[Received November 19, 1964; revised December 24, 1964]